Compression Strength of Composite Primary Structural Components

Semiannual Status Report

Eric R. Johnson
Principal Investigator

Performance Period: May 1, 1992 to October 31, 1992

NASA Grant NAG-1-537

Aerospace and Ocean Engineering Department
Virginia Polytechnic Institute and State University
Blacksburg, Virginia 24061-0203

October, 1992

Technical Monitor: Dr. James H. Starnes, Jr., Head
Aircraft Structures Branch
National Aeronautics and Space Administration
Langley Research Center
Hampton, Virginia 23681-0001

Research Accomplished

Analysis for Delamination Initiation in Postbuckled Dropped-ply Laminates

Objective and background

The objective of this study is analyze the geometrically nonlinear response and delamination initiation of compression-loaded dropped-ply laminates. Specimens made from AS4/3502graphite-epoxy tape were tested in axial compression in an earlier study (Curry, Johnson, and Starnes,1986) and a schematic of these specimens is shown in Fig. 1. The specimens differed in width b and in the layup of the dropped plies. Specimen stacking sequences were $[(\pm 45/0/90)_s, D, (\pm 45/0/90)_s]_T$, in which a zero degree lamina is parallel to the x-axis (load axis) and D denotes the layup of the dropped plies. Hence, the layup of the thin section of the specimen was fixed to be a quasi-isotropic laminate sixteen plies thick. The thick section, which contained the dropped-ply sublaminate, varied from eighteen to twenty-four plies thick. Specimens exhibiting a geometrically nonlinear response to delamination initiation had width b equal to 3.0 in (7.62 cm).

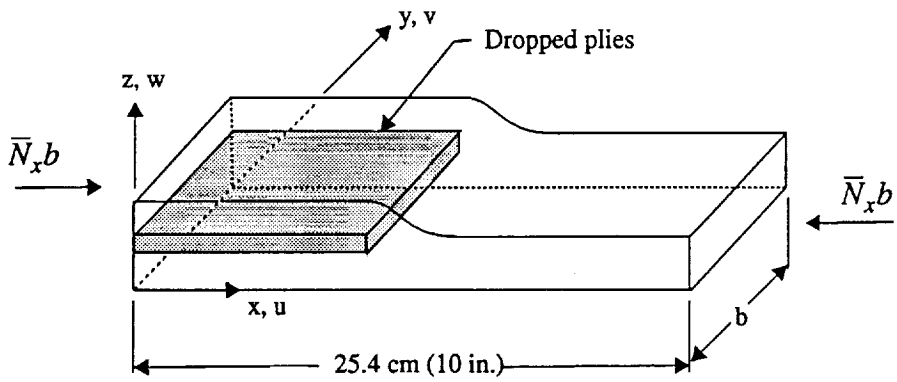

Fig. 1 Schematic of AS4/3502 graphite/epoxy dropped-ply laminated plates tested in axial compression by Curry, et al., 1986.

Recent publications

Work continued on two publications that document the analyses for those specimens that delaminated at the dropped ply site. The references for, and the status of these papers are:

- Dávila, Carlos G., and Johnson, Eric R., "Analysis for Delamination Initiation in Postbuckled Dropped-Ply Laminates," *AIAA Journal*, Paper J20239, accepted for publication July 25, 1992.
- Johnson, Eric R., and Dávila, Carlos G., "Geometrically Nonlinear Transition Elements for Laminate Models Containing Interlaminar Stress Risers," *Composites Engineering*,

submitted July 27, 1992 and under revision.

Copies of these publications have been sent to the technical monitor.

Analysis of the [90_2] dropped-ply specimen

The compression test of a [90_2] dropped-ply specimen (designated as number 6-2 in the report by Curry, Johnson, and Starnes, 1986) resulted in failure initiation by delamination at the intersection of the free edge and the nodal line in the thin section of the laminate at a load of 10,400 lb ($\bar{N}_x$ = 3, 467 lb/in.). The ultimate load of this specimen was 11,219 lbs. Specimens with stiffer dropped-ply sublaminates delaminated at the drop-off site, and many of the [90_n], n= 2, 4, 8, dropped-ply specimens failed in the end grips. Thus, the failure initiation site for this particular [90_2] dropped-ply specimen is somewhat unique.

A schematic of the finite element modeling scheme for specimen 6-2 is shown in Fig. 2. Solid and transition elements are used in the designated shaded region of this figure, which is adjacent to the free edge at the nodal line location in the thin section of the laminate. Since symmetry of the model about the line y = b/2 is assumed, only one free edge region of solid elements is included in the model. The region of solid elements constitutes 5.3% of the planform area in Fig. 2, and the remaining area is modeled with shell/plate elements. The elements used in the COMET software system are: a nine-noded assumed natural strain shell/plate element EX97, a twenty-noded serendipity brick element BR20, and a twelve-noded (TR12) and a fifteen-noded (TR15) transition element for the connection of the brick elements to the shell/plate elements.

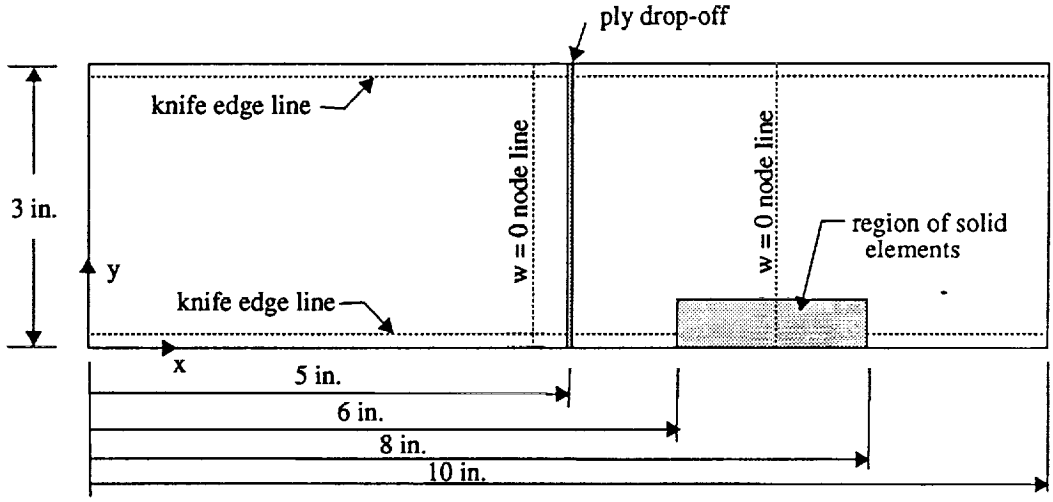

Fig. 2 Plan view of the [90_2] dropped-ply sublaminate specimen 6-2 with approximate locations of the nodal lines for the out-of-plane displacement and the region of solid elements indicated. Shell/plate elements are used for the remainder of the laminate model.

Six BR20 elements span the thickness in the solid element region as shown in Fig. 3. Since there are sixteen plies in this region, some of the elements span a sublaminate. Effective three-dimensional moduli are used to compute element stiffnesses in these cases where one finite ele-

ment includes more than one lamina. These effective moduli are calculated by the LAU processor in COMET. A theory for three-dimensional modeling is presented by Sun and Li (1988). The material properties used for AS4/3502 are given in Table 1. The ply thickness used for the thin section is 0.00543 inches and for the thick section the ply thickness is 0.00544 inches. These thickness values were determined from measurements of specimen 6-2.

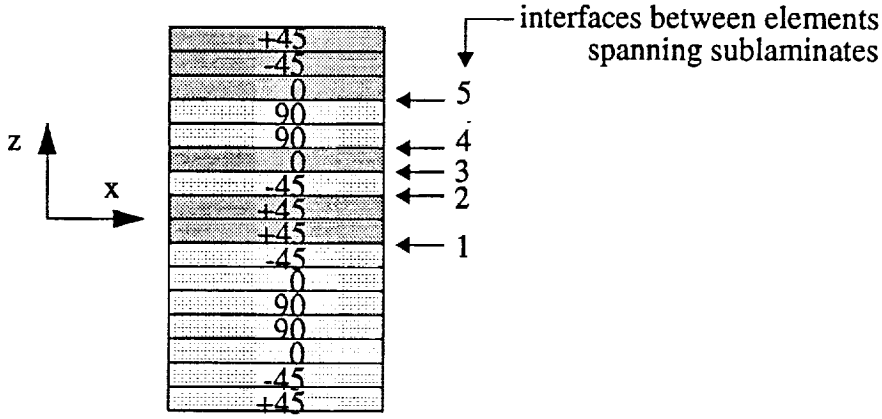

Fig. 3 Six brick elements span the thickness of the sixteen ply laminate in the solid element modeling region. An element occupies a lamina or sublaminate as indicated by the six shaded regions.

TABLE 1. Material properties and strength allowables assumed for AS4/3502 graphite/epoxy unidirectional tape and neat resin

	AS4/3502 graphite/epoxy		
E_1	126 GPa	18.5 Msi	Young's modulus in fiber direction
E_2	11.3 GPa	1.64 Msi	Young's modulus in matrix direction
E_3	11.3 GPa	1.64 Msi	Young's modulus in thickness direction
υ_{12}	0.3		Major Poisson's ratio in 1-2 plane
υ_{13}	0.3		Major Poisson's ratio in 1-3 plane
υ_{23}	0.3		Poisson' ratio in 2-3 plane
G_{12}	6.0 Gpa	0.87 Msi	Shear modulus in 1-2 plane
G_{13}	6.0 GPa	0.87 Msi	Shear modulus in 1-3 plane
G_{23}	3.38 GPa	0.49 Msi	Shear modulus in 2-3 plane
	Neat Resin		
E	3.45 GPa	0.50 Msi	Young's modulus
υ	0.41		Poisson's ratio
G	1.34 GPa	0.195 Msi	Shear modulus
	Interlaminar Strengths		
Z^{S1}	93.1 MPa	13.5 Ksi	Longitudinal shear strength
Z^{S2}	93.1 MPa	13.5 Ksi	Transverse shear strength
Z^T	52.0 MPa	7.54 Ksi	Tensile strength

The load is a uniform axial compressive displacement prescribed at the thick end, and the thin end is fixed. Knife edges run the laminate's length 0.125 inches inboard of the free edge, and this condition is modeled by setting the out-of-plane displacement to zero for the shell elements along the knife edge line (see Fig 2). For each of the short ends, the out-of-plane displacement is prescribed to vanish 0.375 inches into the specimen to simulate the clamped end fixtures of the test.

Numerical results are presented for a finite element model consisting of 72 EX97 shell elements, 180 BR20 solid elements, 96 TR15 transition elements, and 12 TR12 transition elements. The total number of active degrees of freedom is 5,263. A total Lagrangian formulation is employed along with Newton's method to solve for the geometrically nonlinear response.

Interlaminar stresses from the nonlinear finite element analysis are used to compute a dimensionless delamination index F. This index is defined by

$$F = \left(\frac{\tau_{zx}}{Z^{S1}}\right)^2 + \left(\frac{\tau_{zy}}{Z^{S2}}\right)^2 + \left(\frac{\tau_{zz}}{Z^{T}}\right)^2 \qquad \tau_{zz} > 0 \tag{1}$$

in which τ_{zz} is the interlaminar normal stress component, and τ_{zx} and τ_{zy} are interlaminar shear stress components. The strength allowables Z^{S1}, Z^{S2}, and Z^{T} assumed for AS4/3502 are given in Table 1. If the index F equals or exceeds unity, then failure by delamination is assumed to have initiated. However, at stress risers like the free edge of a laminate where interlaminar stress singularities are likely to occur in an elasticity solution to effective modulus models, the peak value of F is meaningless. For finite element approximations to singular elasticity solutions, peak values of F at the stress riser increase monotonically with increasing mesh refinement. Hence the application of a point stress criterion like Eq. (1) has to be modified when singular behavior is expected. In the case of singular behavior, interlaminar stresses from the finite element analysis may be average over some distance from the stress riser and these average values used in Eq. (1). The application of Eq. (1) with averaged stresses was used by Brewer and Lagace (1988) as a delamination criterion. We (Dávila and Johnson, 1992) used Eq. (1) with stresses evaluated at a distance d from the ply drop-off as a delamination criterion. Singular behavior is expected in the analysis of specimen 6-2, so the distributions of F from the finite element analysis can be expected to exceed unity at loads near the experimental failure initiation load.

The results from the finite element analysis at 3,433 lb/in. compression are shown in Figs 4-8. This is the load increment from the analysis just below the experimental failure load of 3,467 lbs/in. The delamination index is plotted over the interface between the -45 degree ply and the +45 degree ply in Fig. 4, which corresponds to interface 1 in Fig. 3. This interface had the largest magnitude of F of the six interfaces where F was evaluated. For the distribution shown in Fig. 4, F_{max} = 1.073 at y = 0 (free edge) and x = 6.778 inches. Also, F = 1 at x = 6.778 when y = 0.0063 inches in Fig. 4. At a load of 3,516 lbs/in, which is the load increment in the analysis just above the experimental failure load, F = 1 at y = 0.0095 inches. Thus, by interpolation the characteristic distance d inward from the free edge for which Eq. (1) would be used to predict delamination initiation is about 0.0076 inches, or d is equal to approximately 1.4 ply thicknesses.

The individual interlaminar stress components which determine the F-distribution in Fig. 4 are shown in Figs. 5-7. Examination of these figures show that the stress component τ_{zx}, the interlaminar shear stress component tangent to the free edge, is the largest contributor to F. Since τ_{xz} is substantially larger than τ_{zz} and τ_{zy} at the free edge in this interface (compare Fig. 6 to Figs. 5 and 7), it is likely that τ_{zx} initiates delamination in the -45/+45 interface at the intersection of the nodal line with the free edge in the thin section of the dropped-ply laminate.

Finally, the influence of the geometric nonlinearity on the interlaminar stress distribution can be illustrated by computing the delamination index from a linear analysis at the same free edge location as used for the geometrically nonlinear analysis for specimen 6-2. The linear analysis

results differs from the nonlinear results in that only one nodal line in the out-of-plane displacement occurs rather than the two nodal lines in the nonlinear response. The one nodal line in the linear analysis occurs near the ply drop-off, and no nodal line occurs in the thin section. The distribution of the delamination index F at interface 2 (see Fig. 3) from the linear analysis is shown in Fig. 8 at a compressive load of 3,433 lb/in. Interface 2 had a larger peak value of F than interface 1. Comparing Figs. 4and 8, it can be seen that a linear analysis substantially underpredicts the interlaminar stress intensity for specimen 6-2.

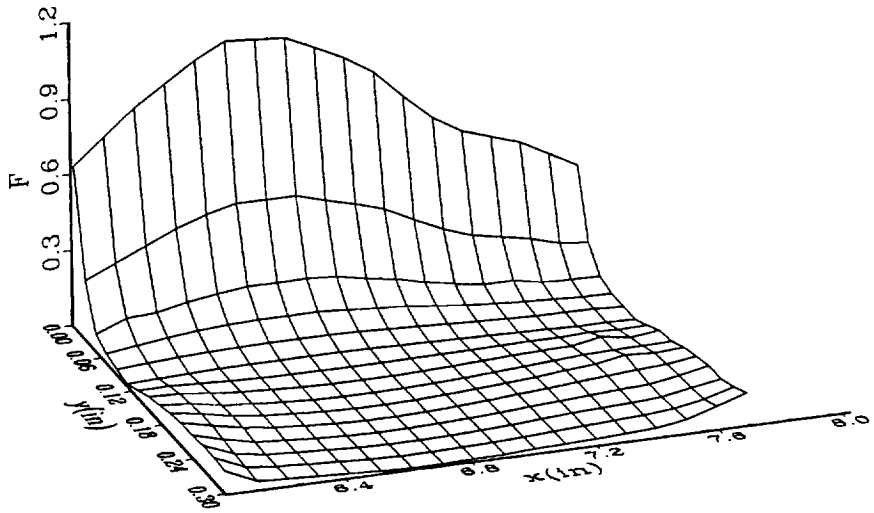

Fig. 4 Distribution of the delamination index F in the -45/+45 interfacial plane (interface 1 in Fig. 3) of specimen 6-2 from the nonlinear analysis at a compressive load of 3,433 lb/in. Free edge at y = 0 and knife edge support at y = 0.125 in.

Graduate research assistant

Ms. F. Aylin Barlas is the graduate assistant on this project, and this work is the basis for her master's thesis in Aerospace Engineering.

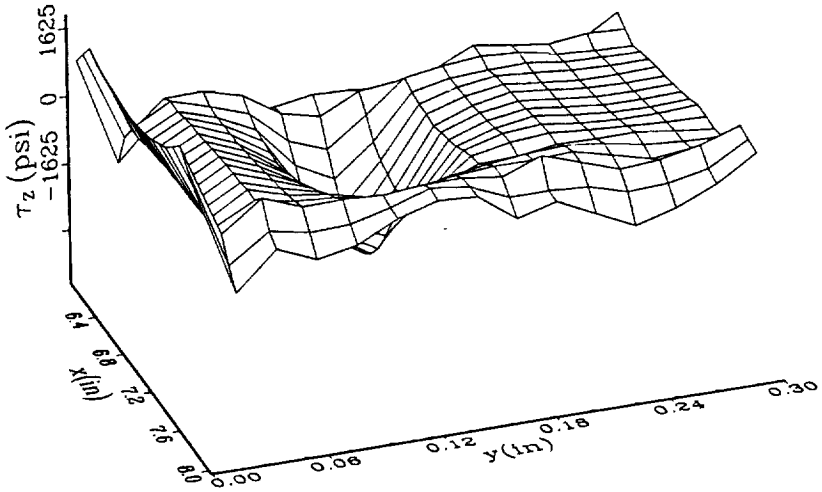

Fig. 5 Distribution of the interlaminar normal stress component in the -45/+45 interfacial plane (interface 1 in Fig. 3) of specimen 6-2 from nonlinear analysis at a compressive load compressive load of 3,433 lb/in. Free edge at y = 0 and knife edge support at y = 0.125 in.

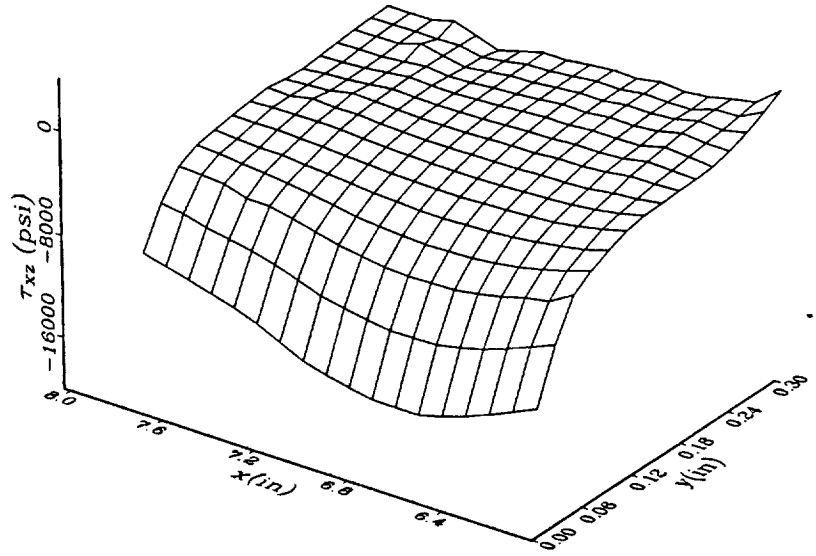

Fig. 6 Distribution of the interlaminar shear stress component tangent to the free edge in the -45/+45 interfacial plane (interface 1 in Fig. 3) of specimen 6-2 from nonlinear analysis at a compressive load of 3,433 lb/in. Free edge at y = 0 and knife edge support at y = 0.125 in.

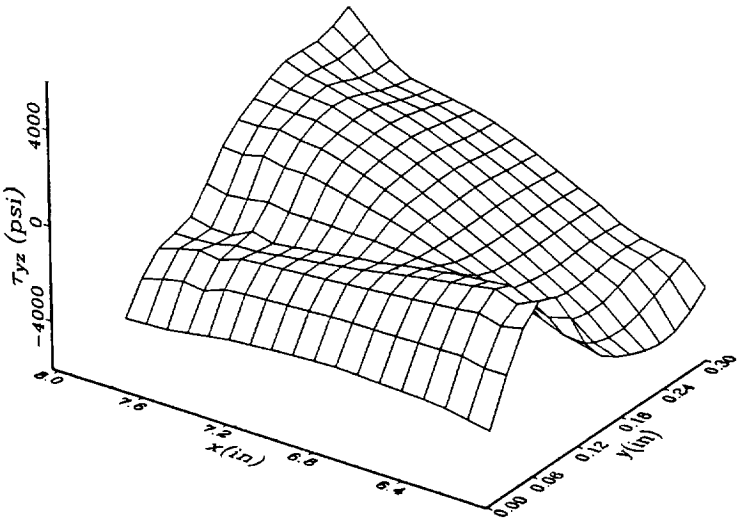

Fig. 7 Distribution of the interlaminar shear stress component normal to the free edge in the -45/ +45 interfacial plane of specimen 6-2 from nonlinear analysis at a compressive load of 3,433 lb/in. Free edge at y = 0 and knife edge support at y = 0.125 in.

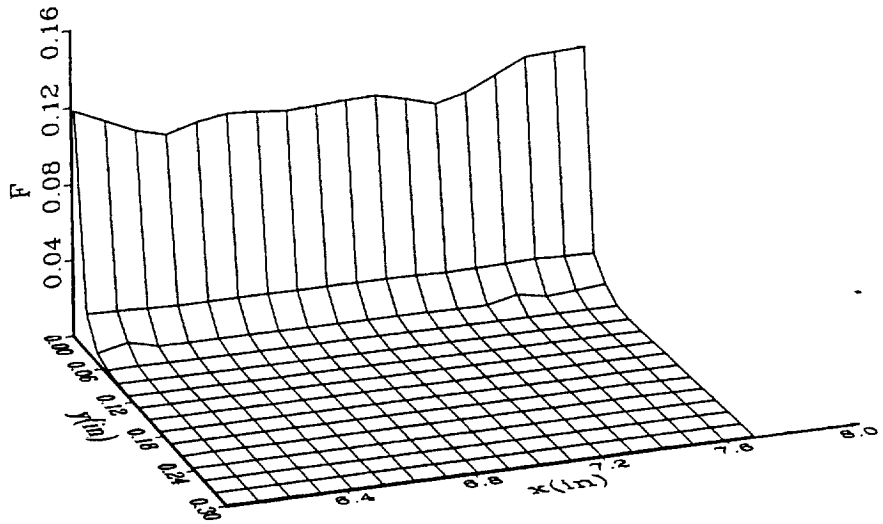

Fig. 8 Distribution of the delamination index F in the +45/-45 interfacial plane (interface 2 in Fig. 3) of specimen 6-2 from linear analysis at a compressive load of 3,433 lb/in. Free edge at y = 0 and knife edge support at y = 0.125 in.

Stiffener Crippling Initiated by Delamination

Background and objective

Graphite-epoxy stiffeners tested in compression (Bonanni, Johnson, and Starnes, 1991) showed evidence of failure initiation in postbuckling by delamination at the free edges of the flanges. This mode of failure initiation occurred in *I*- and *J*-section specimens with flange width to thickness ratios in the range from ten to twenty. The analyses conducted in the Bonanni study modeled the stiffeners as a branched shell using the STAGS computer code. Since shell theories are based on plane stress and neglect through-the-thickness stress components, failure initiated by interlaminar stresses at the free edges of the flanges due to bending in postbuckling could not be studied with the STAGS model.

The objective of this project is to develop a computational model of the stiffener specimens that includes the capability to predict the interlaminar stress response at the flange free edge in postbuckling.

I-section specimen

Computational models were developed for the I-section specimen designated *I-2* by Bonanni, et al. (1991). This specimen had an axial gage length of 5.944 inches with an additional inch at each end of the specimen potted into fixtures. The cross section and measured dimensions are shown in Fig. 9 below. Specimens were fabricated from AS4/3502 graphite/epoxy unidirectional tape with material properties listed in Table 1. The wall construction was eight plies of tape with a $[\pm 45/0/90]_s$ stacking sequence in the web and two diagonally opposite flanges. The stacking sequence in the two other flanges is $[\pm 45/0/90_2/0/\pm 45]_T$, because of the fabrication process with tape sublaminates. Crippling for specimen *I-2* initiated due to a local material compressive strength failure in the corner where the flanges and web meet and not due to flange free edge delamination. However, the detailed STAGS results reported by Bonanni et al. (1991) for specimen *I-2* provides a good benchmark to assess current modeling techniques. Once current modeling techniques are established for this benchmark case, then this experience will guide the modeling of specimens that did initiate crippling by flange free edge delamination.

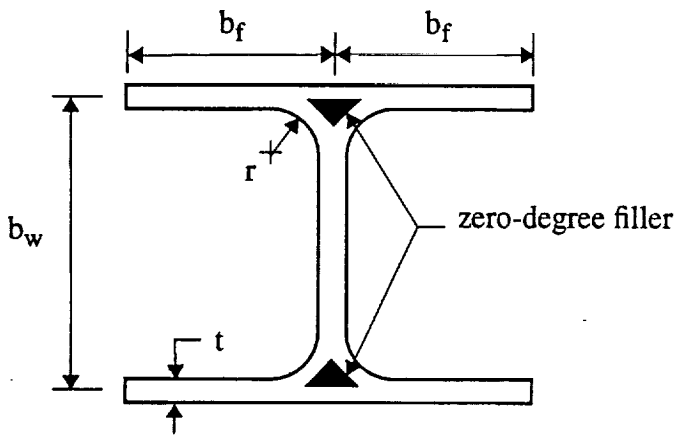

Dimensional data
t = 0.0455 inches
b_f = 1.262 inches.
b_w = 1.247 inches
r = 0.125 inches

Fig. 9 Specimen *I-2*

Computational modeling

A geometrically nonlinear finite element model is being developed using the COMET software system. The model consists of nine-noded EX97 shell/plate elements, transition elements TR12 and TR15, and twenty-noded solid elements BR20. The solid elements are used in a local region near the flange free edge to estimate the interlaminar stresses. They are connected to transition elements which in turn are connected to the shell elements. Shell/plate elements are used in the majority of the stiffener. Thus, the solid elements are only used in regions where three-dimensional effects are important, and this is a significant modeling strategy because a stiffener modeled with all solid elements is not warranted based on the mechanics and is prohibitively large computationally. This issue of very large degree-of-freedom numerical models is compounded in nonlinear analysis because of the iterative nature of the solution procedure.

Two shell models were examined initially; i.e., no solid element subdomains were included. Both models used EX97 plate elements in the four flanges and web. It is at the junctions of the web to flanges where the two models differed. As shown in Fig. 9, the actual specimen had zero-degree tape inserted into the junctions to fill the void created by sublaminate fabrication the specimens. This creates a stiff insert in the corner junctions. Model I use E210 beam elements to represent the stiff insert, and Model II used narrow-width plate elements with a zero-degree unidirectional layup properties to represent the stiff insert. A bifurcation buckling analysis was performed for the purely compressive prebuckling equilibrium configuration. Model I had 3,925 active degrees of freedom and Model II had 4,515 active degrees of freedom. The results for the load-end shortening stiffness in prebuckling equilibrium K_{pb} and the bifurcation buckling load P_{cr} are shown in Table 2 along with experimental results. The results attained with Model II are slightly better than with Model I. However, Model II had longer CPU times to converge relative to Model I because of its increased number of degrees of freedom relative to Model I. Model I was close enough to the experiment to select it for further nonlinear analysis.

Table 2: Prebuckling stiffness K_{pb} and bifurcation buckling load P_{cr} from two finite element models of specimen *I-2* compared to experiment

	K_{pb}, lb/in.	P_{cr}, lb.
Model I[a]	282,800	2,931
Model II[b]	302,193	2,708
Experiment (Bonanni, et al, 1991)	296,450	2,786

a. For shell elements E_1 = 17 Msi, and for beam elements E = 10 Msi.
b. For all shell elements E_1 = 18. 5 Msi.

Models I and II were used in a geometrically nonlinear analysis by including an initial shape imperfection in the pattern of the buckling mode with a maximum amplitudes of one-tenth of the flange thickness. The load-end shortening plot from these analyses is shown in Fig. 10 along with the experimental results. Both models agree very well with the experimental results. Model II results are only shown to a compressive load magnitude slightly greater than 6,000 lbs, since it converges more slowly than Model I. These nonlinear results again indicate that the shell/plate Model I is adequate to capture the load-shortening response of specimen I-2.

Adding a reasonable number of solid elements in a subdomain at the free edge of a flange for Model I increased the degrees of freedom from 3,925 in the shell/beam model to over 5,500 for the solid/shell/beam model. Since we are only interested in computing interlaminar stresses near the experimental failure load, and the shell/beam model is apparently sufficient to capture the geometrically nonlinear response, we propose to do variable complexity modeling. That is, a nonlinear analysis is carried out on the shell/beam model (3,925 degrees of freedom) to a load near failure initiation in the experiment. Then, the complexity of the model is changed to include the subdomain of solid elements, an additional 1,500 degrees of freedom or so. Since Newton's method is based on a good initial guess to the solution, shell kinematics may be employed to estimate the three displacements of each node in the solid element subdomain. With this initial guess, Newton's method is initiated for the complex solid/shell/beam model. Hopefully, we can converge at the last successful load step of the shell/beam model with only one sequence of Newton's iterations for the complex model at this same load. This strategy requires more programming in the COMET software system than attempted to date. Displacement data files have to created from the shell/beam model that are applicable to the solid/shell/beam model, so that a restart of the NL_STATIC_1 procedure on the complex model can be initiated. We have worked-out the programming details on simpler problems involving variable complexity modeling, and are in the process of applying these programming steps to the I-section model.

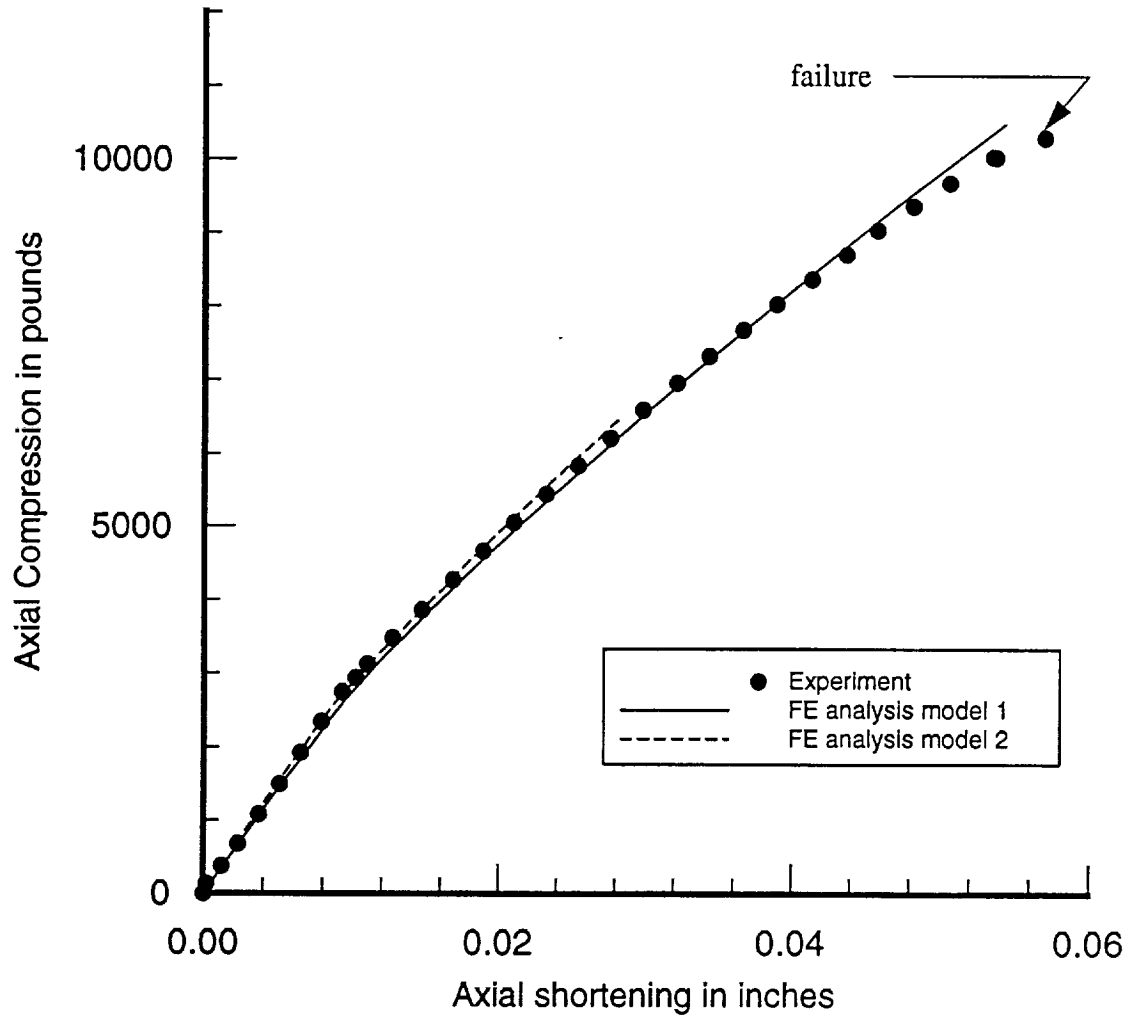

Fig. 10 Load-end shortening for specimen I-2 compared to two finite element models of its response.

Graduate research assistant

Ms. F. Aylin Barlas is the graduate assistant on this project, and this work is the basis for her master's thesis in Aerospace Engineering.

Pressure Pillowing of an Orthogonally Stiffened Cylindrical Shell

Objective and background

This project is motivated by the application of advanced composite materials in the construction of fuselage primary structure for transport aircraft. We consider a laminated composite material cylindrical shell internally stiffened by a regular arrangement of stringers and frames, or rings, and subjected to internal pressure and axial load. The objective is to determine the distribution of the interacting loads between the stiffeners and the shell wall; particularly the load transfer at the stiffener crossing point.

Summary of approach

For the mathematically infinite length circular cylinder, a structural repeating unit is defined that consists of a portion of the shell wall centered over the stringer and frame intersection. See Fig. 11. The shell is modeled with Sander's theory, and the stiffeners are modeled with Vlasov's thin-walled bar theory extended to composite material construction. The principle of virtual work is employed for each structural element, and the assumed 3 X 1 displacement vector functions u for each element is the sum of a principal part u_p, a particular part u_P, and a Fourier Series part u_{fs}. In the shell, for example, the principal part of the displacement vector contains exponentially decaying functions which account for the jump in the stress and moment resultants at the stiffener connections, the particular part accounts for stretching under axial load, and the Fourier Series part is periodic in the frame and stringer spacing. Inter-element continuity is enforced by augmenting the virtual work functional with integrals of Lagrange multiplier functions times variations in the displacement constraints. The Lagrange multipliers are interpreted as the components of the line loads between the stiffeners and shell, and they are expanded in a Fourier Series as well. Augmented virtual work leads to a set of equilibrium equations for the displacement and Lagrange multiplier coefficients. The displacement constraint equations are enforced by the vanishing of the inner product of these equations with the variations in the Lagrange multiplier functions. The complete set of equations for the displacement and Lagrange multiplier coefficients is indeterminate, but can be solved by first eliminating the displacement sub-vector and then solving for the Lagrange multiplier sub-vector.

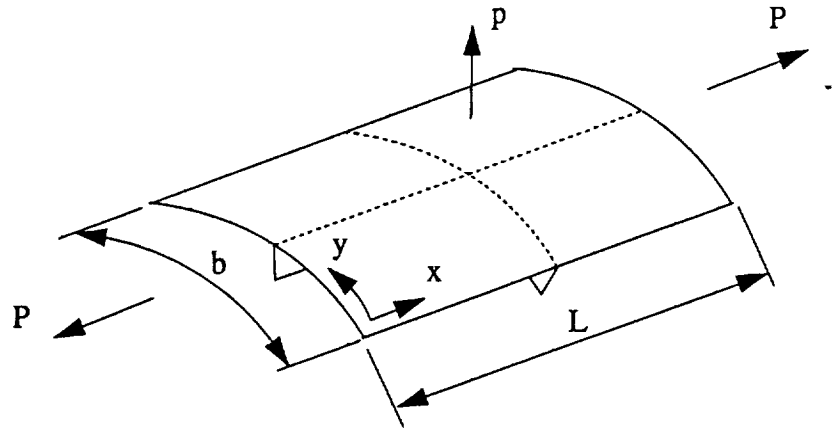

Fig. 11 Repeating unit of an orthogonally stiffened cylindrical shell subject to internal pressure p and axial load P.

Preliminary results

We are comparing the results of our model to those published by Wang and Hsu (1985). Wang and Hsu give results for a balanced, symmetrically laminated skin with a 117.5 inch radius, a 20 inch frame spacing (L = 20), a 5.8 inch stringer spacing (b = 5.8), and for an internal pressure p of 10 psi. They include closed-end pressure vessel effect which implies that the axial load P = 3,407.5 lb on a generic repeating unit. The results presented below include the Fourier series portion of the assumed displacement fields and the particular part to account for axial stretching. The principal part of the displacement field that accounts for jump conditions in the shell in-plane shear and Kirchhoff shear at the stiffener attachment lines are not included. The Fourier Series expansions were truncated at twenty-four harmonic terms in the axial and circumferential directions.

The distributions of the out-of-plane displacements of the skin from our solution are shown in Figs. 12 and 13. These displacements compare very well to those presented by Wang and Hsu (see their Fig. 5). Axial strain distributions on the inner and outer surfaces of the skin at an internal pressure of 10 psi are shown in Fig.14, and the circumferential strain distributions on the surfaces of the skin are shown in Fig. 15. These strain distributions do not agree with those presented by Wang and Hsu (see their Figs. 6 and 7). For example, the axial strain distribution in the circumferential direction from our results (Fig. 14) starts at about 2000$\mu\varepsilon$ at x = 0 and y =0 and remains the same value to x = 0 and y = b/2. The corresponding strain distribution from Wang and Hsu's results is about 2700$\mu\varepsilon$ at x =y = 0 and decreases to about 45$\mu\varepsilon$ at x = 0 and y = b/2. The decrease in axial strain from 2700$\mu\varepsilon$ to 45$\mu\varepsilon$ is attributed to the present of the stringer at y = b/2, and it is clear our results do not capture this influence. We believe that including the principal part of the shell displacement field will help alleviate this discrepancy, and we are also investigating if the particular part of the displacement field that accounts for stretching due to axial load is sufficiently general. The trends in the remaining strain distributions shown in Figs. 14 and 15 are similar to Wang and Hsu's results but do not agree quantitatively.

An interesting result not published by Wang and Hsu, is the distribution of the interacting line loads between the skin and stiffeners. The normal and tangential components of the line load between the stringer and skin are shown in Figs. 16 and 17, respectively. The corresponding components between the frame and skin are shown in Figs. 18 and 19. The normal components of these line loads exhibit delta function behavior, and the tangential components exhibit step function behavior, at the stiffener crossing point. Although the results are not presented here, it was observed that increasing the number of terms in the Fourier series, within a range limited by computer resources, caused increasing peak magnitudes of the normal line loads at the crossing point. This interesting result suggests that we should include displacement fields to account for singularities in the force and moment resultants in the skin, and point forces at the crossing point in the Lagrange multiplier distribution.

Graduate research assistant

Naveen Rastogi is the graduate assistant on this project, and this work is the basis of his dissertation for the Doctor of Philosophy degree in Aerospace Engineering.

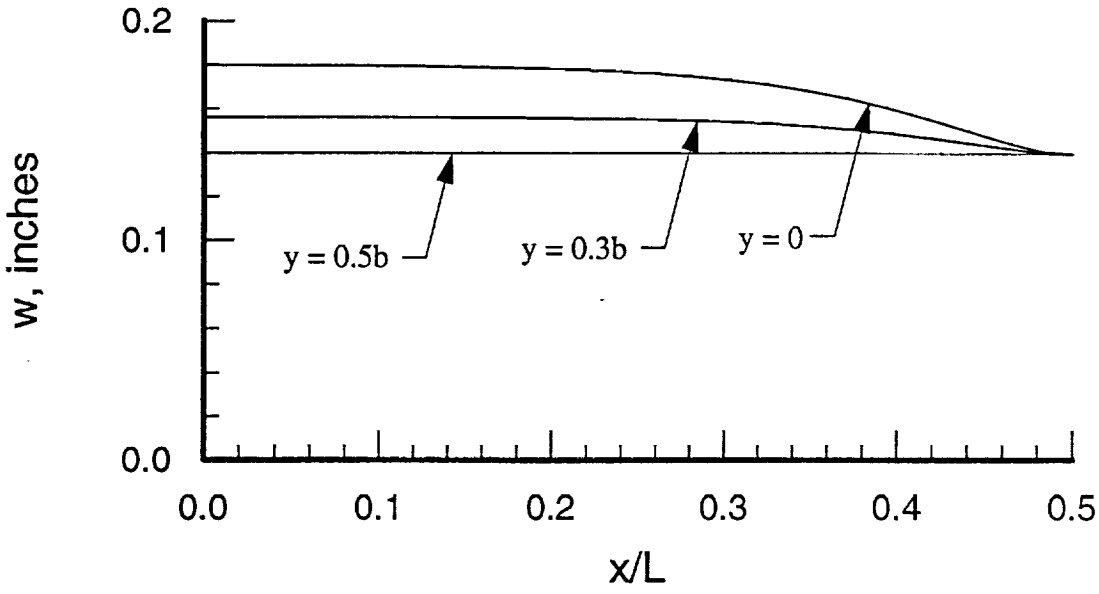

Fig. 12 Axial distributions of the out-of-plane displacement of the skin at three circumferential positions at an internal pressure of 10 psi.

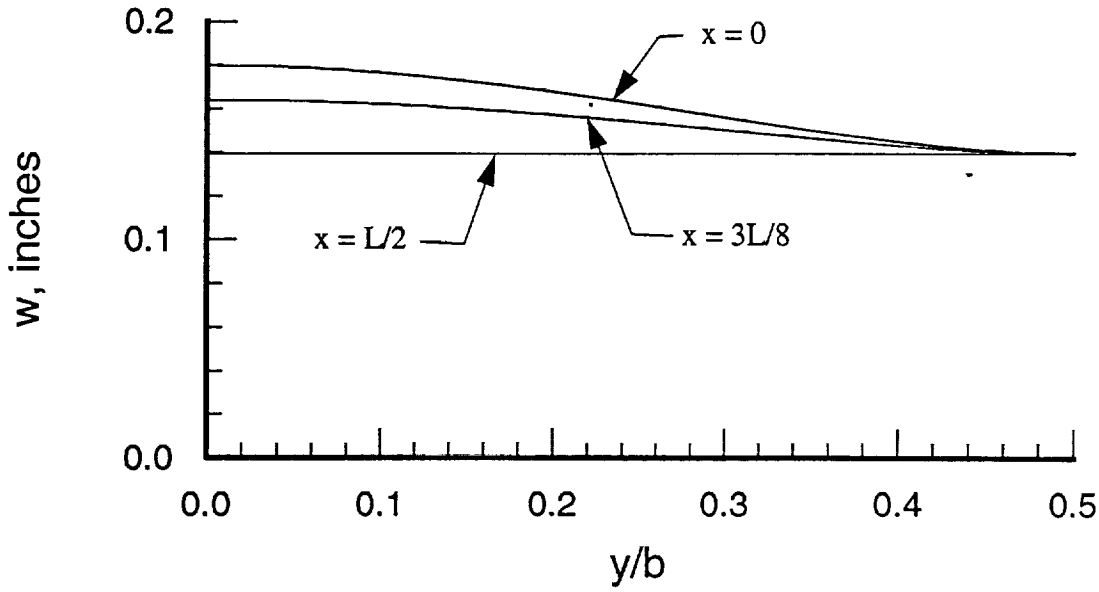

Fig. 13 Circumferential distributions of the out-of-plane displacement of the skin at three axial locations at an internal pressure of 10 psi.

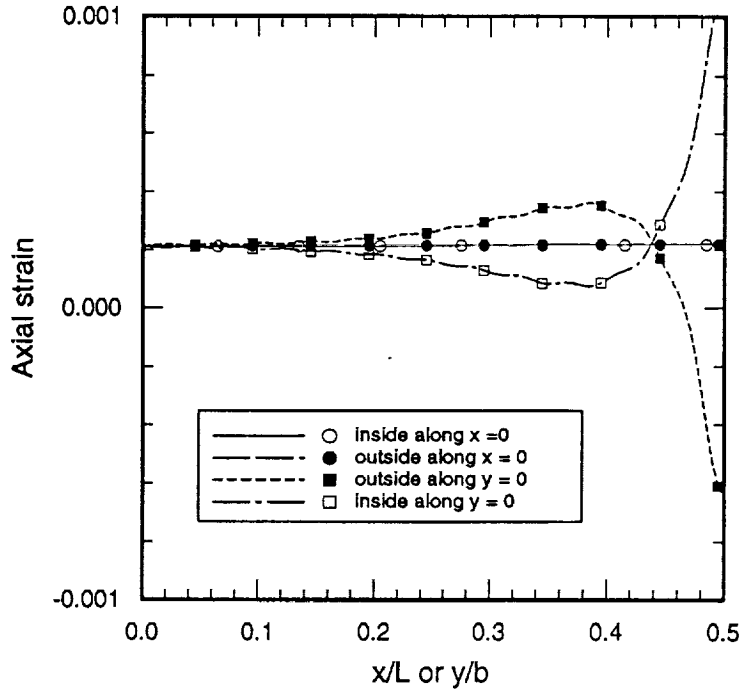

Fig. 14 Axial normal strain distributions on the skin surfaces at an internal pressure of 10 psi.

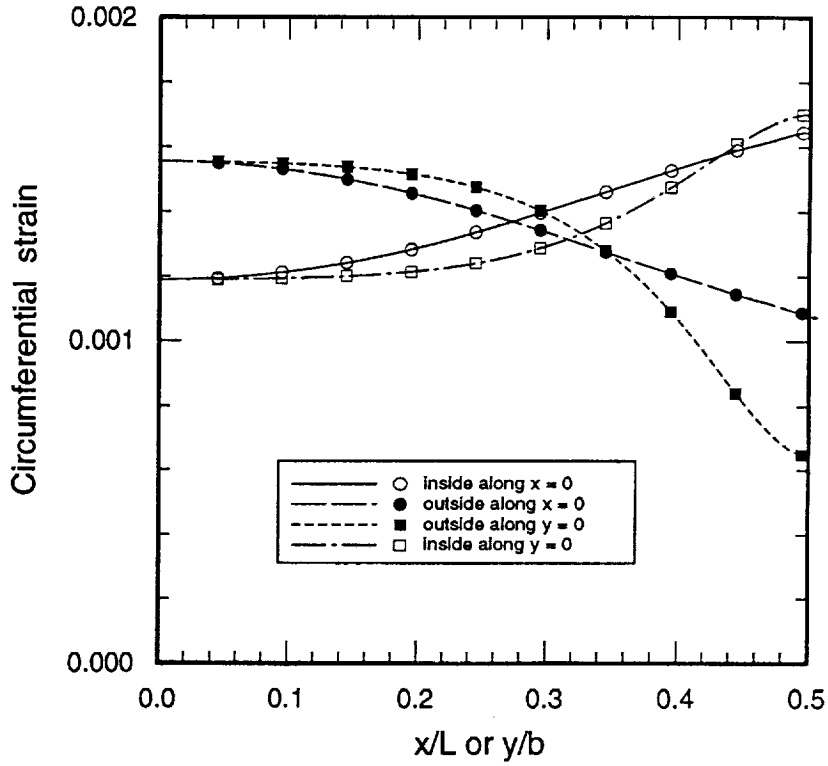

Fig. 15 Circumferential strain distributions on the skin surfaces at an internal pressure of 10 psi.

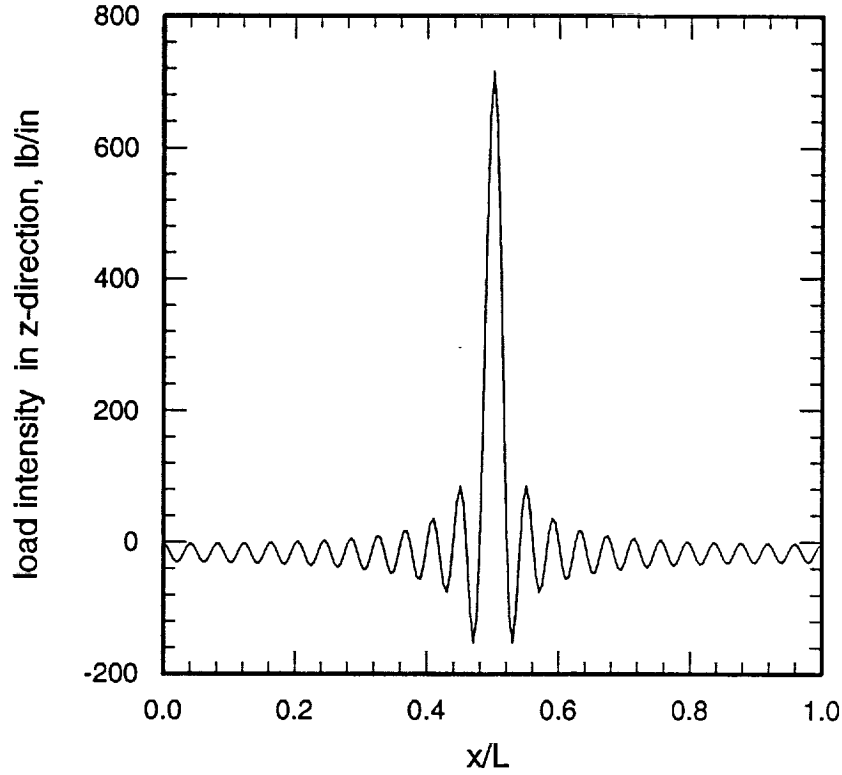

Fig. 16 Normal load intensity between the stringer and skin at an internal pressure of 10 psi.

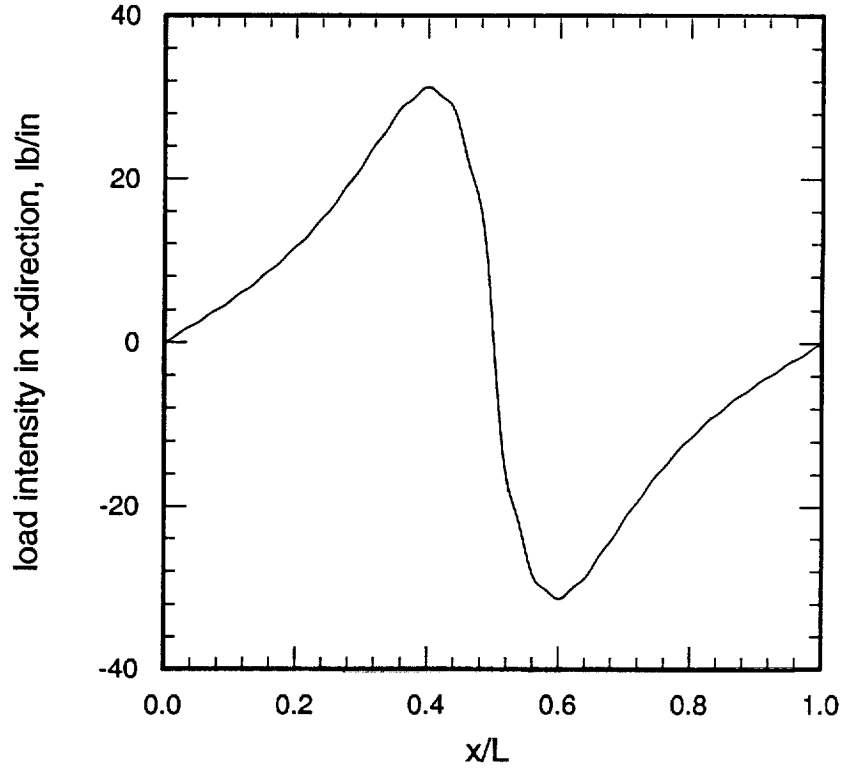

Fig. 17 Tangential load intensity between stringer and skin at an internal pressure of 10 psi.

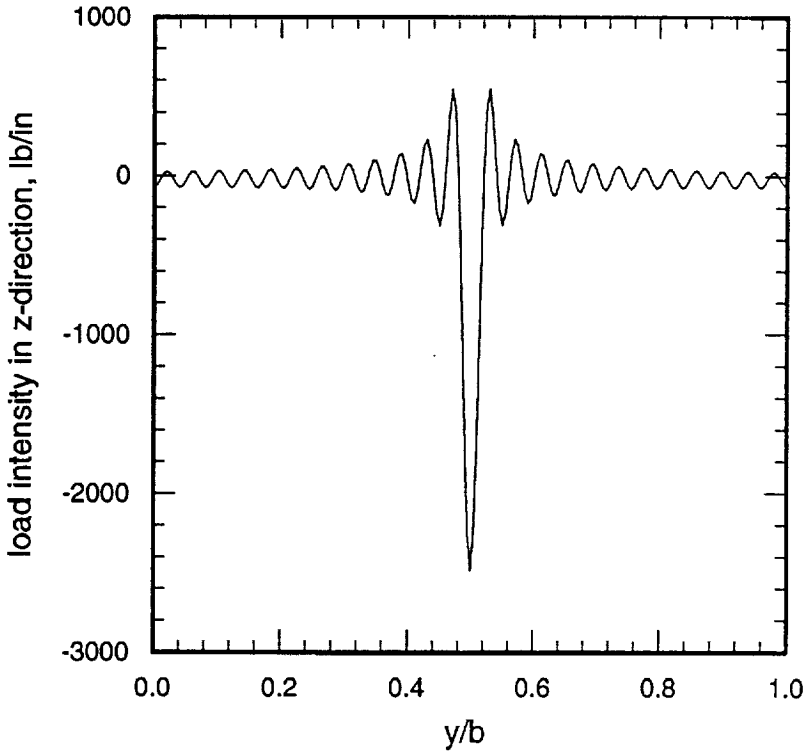

Fig. 18 Normal load intensity between frame and skin at an internal pressure of 10 psi.

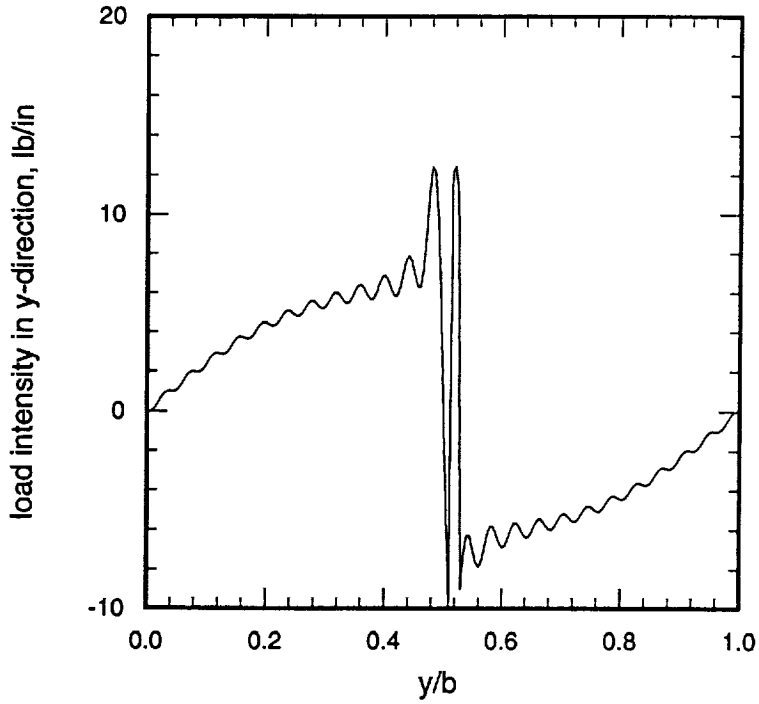

Fig. 19 Tangential load intesity between frame and skin at an internal pressure of 10 psi.

References

Bonanni, David L., Johnson, Eric R., and Starnes, James H., Jr., 1991, "Local Crippling of Thin-Walled Graphite-Epoxy Stiffeners", *AIAA Journal*, Vol. 29., No. 11, November, pp. 1951-1959.

Brewer, J. C., and Lagace P. A., 1988, "Quadratic Stress Criterion for Initiation of Delamination," *Journal of Composite Materials*, Vol. 22, December, pp. 1141-1155

Curry, J. M., Johnson, E. R., and Starnes, J. H., Jr., 1986, "Effect of Ply Drop-Offs on the Strength of Graphite-Epoxy Laminates," Center for Composite Materials and Structures, Virginia Polytechnic Inst. and State Univ., Blacksburg, VA 24061, Rept. CCMS-86-07 and VPI-E-86-27, December.

Sun, C. T., and Li, Sijan, 1988, "Three-Dimensional Effective Elastic Constants for Thick Laminates," *Journal of Composite Materials*, Vol. 22, July, pp. 629-639.

Wang, J. T-S, and Hsu, T-M, 1985, "Discrete Analysis of Stiffened Composite Cylindrical Shells," *AIAA Journal*, Vol. 23, No. 11, November, pp. 1753-1761.

Accumulative data for Grant NAG-1-537
November 1, 1984 to October 31, 1992

Publications Sponsored Under the Grant

Journal Papers

1. Bonanni, David L., Johnson, Eric R., and Starnes, James H., Jr., "Local Crippling of Thin-Walled Graphite-Epoxy Stiffeners", *AIAA Journal*, Vol. 29., No. 11, November 1991, pp. 1951-1959.

2. Curry, James H., Johnson, Eric R., and Starnes, James H., Jr., "Effect of Dropped Plies on the Strength of Graphite-Epoxy Laminates," *AIAA Journal*, Vol. 30, No.2, February 1992, pp. 449-456.

3. Dávila, Carlos G., and Johnson, Eric. R., "Analysis for Delamination Initiation in Postbuckled Dropped-Ply Laminates," *AIAA Journal*, Paper J20239, accepted for publication July 25, 1992.

Conference Papers

1. Lo, Patrick K-L, and Johnson Eric. R., "One-Dimensional Analysis of Filamentary Composite Beam Columns with Thin-Walled Open Sections," in ***Composites '86: Recent Advances in Japan and the United States***, K. Kawata, S. Umekawa & A. Kobayashi, Eds., Proceedings of the Third Japan-U.S. Conference on Composite Materials, Japan Society For Composite Materials, 1986, pp. 405-414. (Supported in part by NASA Grant NAG-1-343.)

2. Curry, James M., Johnson, Eric R., and Starnes, James H., Jr., "Effect of Dropped Plies on the Strength of Graphite-Epoxy Laminates," AIAA Paper No. 87-0874, in the proceedings of the *AIAA/ASME/ASCE/AHS 28th Structures, Structural Dynamics and Materials Conference*, Part 1, April 6-8, 1987, Monterey, California, pp. 737-747.

3. Bonanni, David L., Johnson, Eric., R., and Starnes, James H., Jr., "Local Crippling of Thin-Walled Graphite-Epoxy Stiffeners," AIAA Paper No. 88-2251, in the proceedings of the *AIAA/ASME/ASCE/AHS 29th Structures, Structural Dynamics and Materials Conference*, Part 1, April 18-20, 1988, Williamsburg, Virginia, pp. 313-323. (Supported in part by NASA Grant NAG-1-343.)

4. Johnson, E. R., and Bonanni, D. L., "Order 2p Derivatives from p-Differentiable Finite Element Solutions by a Spectral Method," in ***CAD/CAM, Robotics and Factories of the Future***, Vol. 1, Birendra Prasad, Ed., Springer-Verlag, Berlin, 1989, pp. 134-138.

5. Johnson, Eric R., and Dávila, Carlos G., "Compression Buckling of Thick Orthotropic Plates with a Step Thickness Change," in the *Proceedings of the Twelfth Canadian Congress of Applied Mechanics*, Carleton University, Ottawa, Canada, M. A. Erki and J. Kirkhope, Eds., Vol. 1, 28 May - 2 June, 1989, pp. 140 & 141.

6. Haftka, Raphael T., and Johnson, Eric R., "Initial Postbuckling Response of an Unsymmetrically Laminated Rectangular Plate," in the Proceedings of the *Eighth DOD/NASA/FAA Conference on Fibrous Composites in Structural Design*, November 28-30, 1989, Norfolk, Virginia, NASA Conference Publication 3087, Part 2, 1990, pp. 609-623. (Supported in part by NASA Grant NAG-1-168.)

7. Dávila, Carlos G., and Johnson, Eric R., "Analysis for Delamination Initiation in Postbuckled Dropped-ply Laminates," AIAA Paper No. 92-2226, in the proceedings of *The 33rd AIAA/ ASME/ASCE/AHS/ASC Structures, Structural Dynamics and Materials Conference*, Part 1, April 13-15, 1992, Dallas Texas, pp. 29-39.

8. Johnson, Eric R., and Haftka, Raphael T., "Initial Postbuckling Response of Anisotropic Laminated Rectangular Plates," AIAA Paper No. 92-2284, in the proceedings of *The 33rd AIAA/ ASME/ASCE/AHS/ASC Structures, Structural Dynamics and Materials Conference*, Part 1, April 13-15, 1992, Dallas Texas, pp. 241-263. (Supported in part by NASA Grant NAG-1-168.)

Presentations

(Speaker indicated by boldface font.)

1. Lo, Patrick K-L, and **Johnson Eric. R.**, "One-Dimensional Analysis of Filamentary Composite Beam Columns with Thin-Walled Open Sections," in Session 10 Compression/Shear, The Third Japan-U.S. Conference on Composite Materials, June 23-25, 1986, Science University of Tokyo, Kagurazaka, Tokyo, Japan.

2. **Curry, James M.**, Johnson, Eric R., and Starnes, James H., Jr., "Effect of Dropped Plies on the Strength of Graphite-Epoxy Laminates," at the *AIAA/ASME/ASCE/AHS 28th Structures, Structural Dynamics and Materials Conference*, April 6-8, 1987, Monterey, California.

3. **Bonanni, David L.**, Johnson, Eric., R., and Starnes, James H., Jr., "Local Crippling of Thin-Walled Graphite-Epoxy Stiffeners," at the *AIAA/ASME/ASCE/AHS 29th Structures, Structural Dynamics and Materials Conference*, April 18-20, 1988, Williamsburg, Virginia.

4. **Johnson, E. R.**, and Bonanni, D. L., "Order 2p Derivatives from p-Differentiable Finite Element Solutions by a Spectral Method," at the *3rd International Conference on CAD/CAM Robotics and Factories of the Future (CARS & FOF '88)*, Southfield, Michigan, August 14-17, 1988.

5. Johnson, Eric R., and **Dávila, Carlos G.**, "Compression Buckling of Thick Orthotropic Plates with a Step Thickness Change," Special Session: Mechanics of Laminated Structures, at the *Twelfth Canadian Congress of Applied Mechanics*, Carleton University, Ottawa, Canada, 28

May - 2 June, 1989.

6. Haftka, Raphael T., and **Johnson, Eric R.**, "Initial Postbuckling Response of an Unsymmetrically Laminated Rectangular Plate," Methodology and Design Session, at the *Eighth DOD/ NASA/FAA Conference on Fibrous Composites in Structural Design*, November 28-30, 1989, The Omni International Hotel, Norfolk, Virginia.

7. **Foster, John L.**, and Johnson, Eric R., "Computation of Interlaminar Stresses From Finite Element Solutions to Plate Theories," Session 35: Work in Progress II, at *The 32nd AIAA/ ASME/ASCE/AHS/ASC Structures, Structural Dynamics and Materials Conference*, April 8-10, 1991, Hyatt Regency Baltimore, Baltimore, Maryland.

8. **Dávila, Carlos G.**, and Johnson, Eric R., "Analysis for Delamination Initiation in Postbuckled Dropped-ply Laminates," Session 5: Damage Tolerance of Composites, at *The 33rd AIAA/ ASME/ASCE/AHS/ASC Structures, Structural Dynamics and Materials Conference*, April 13-15, 1992, Grand Kempinski Hotel, Dallas, Texas.

9. **Johnson, Eric R.**, and Haftka, Raphael T., "Initial Postbuckling Response of Anisotropic Laminated Rectangular Plates," Session 14: Buckling/Postbuckling of Plates and Stiffened Panels, at *The 33rd AIAA/ASME/ASCE/AHS/ASC Structures, Structural Dynamics and Materials Conference*, April 13-15, 1992, Grand Kempinski Hotel, Dallas, Texas.

Reports

1. Curry, J. M., Johnson, E. R., and Starnes, J. H., Jr., "Effect of Ply Drop-Offs on the Strength of Graphite-Epoxy Laminates," Center for Composite Materials and Structures, Virginia Polytechnic Inst. and State Univ., Blacksburg, VA 24061, Rept. CCMS-86-07 and VPI-E-86-27, December 1986.

2. Bonanni, D. L., Johnson, E. R., and Starnes, J. H., Jr., "Local Buckling and Crippling of Composite Stiffener Sections," Center for Composite Materials and Structures, Virginia Polytechnic Inst. and State Univ., Blacksburg, VA 24061, Rept. CCMS-88-08 and VPI-E-88-15, June 1988. (Supported in part by NASA Grant NAG-1-343.)

3. Foster, J. L., and Johnson, E. R., "Computation of Interlaminar Stresses From Finite Element Solutions to Plate Theory," Center for Composite Materials and Structures, Virginia Polytechnic Inst. and State Univ., Blacksburg, VA 24061, Rept. CCMS-91-10 and VPI-E-91-10, June 1991.

4. Dávila, C. G., and Johnson, E. R., "Delamination Initiation in Postbuckled Dropped-ply Laminates," Center for Composite Materials and Structures, Virginia Polytechnic Inst. and State Univ., Blacksburg, VA 24061, Rept. CCMS-91-24 and VPI-E-91-23, December 1991.

5. Dávila, Carlos G. and Johnson, Eric R., "The Computational Structural Mechanics Testbed: User's Manual for Transition Elements in Processor ES16," Aerospace and Ocean Engineering, Virginia Polytechnic Institute and State University, Blacksburg, Virginia 24061-0203, February 1992, (draft).

Students Earning Degrees and Sponsored Under the Grant

1. James M. Curry, Master of Science in Aerospace Engineering, May 1986.
   Thesis Title: Effect of Ply Drop-Offs on the Strength of Graphite-Epoxy Laminates
   Initial Employer: Rohr Industries, Inc., Chula Vista CA

2. David L. Bonanni, Master of Science in Aerospace Engineering, April 1988.
   Thesis Title: Local Crippling of Composite Stiffener Sections
   Initial Employer: David Taylor Research Center, Bethesda MD
   (Supported in part by NASA Grant NAG-1-343.)

3. John L. Foster, Master of Science in Aerospace Engineering, April 1991.
   Thesis Title: Computation of Interlaminar Stresses from Finite Element Solutions to Plate Theory
   Initial Employer: McDonnell Douglas Space Systems Co., Huntington Beach CA.

4. Carlos G. Dávila, Doctor of Philosophy in Aerospace Engineering, November 1991
   Dissertation Title: Delamination Initiation in Postbuckled Dropped-Ply Laminates
   Initial Position: National Research Council Resident Research Associate,
   NASA Langley Research Center, Hampton VA